HHS Public Access

Author manuscript

Int J Obes (Lond). Author manuscript; available in PMC 2019 December 07.

Published in final edited form as:

Int J Obes (Lond). 2019 December ; 43(12): 2434–2447. doi:10.1038/s41366-019-0366-4.

MRP14 enhances the ability of macrophage to recruit T cells and promotes obesity-induced insulin resistance

Chang Xia[1,2], **Michael Razavi**[2], **Xiaoquan Rao**[3], **Zachary Braunstein**[4], **Hong Mao**[5], **Amelia C. Toomey**[6], **Yunmei Wang**[2], **Daniel I. Simon**[2], **Shi Zhao**[4,*], **Sanjay Rajagopalan**[2], **Jixin Zhong**[2,*]

[1]College of Health Science & Nursing, Wuhan Polytechnic University, Wuhan, Hubei 430023, China;

[2]Cardiovascular Research Institute, Case Western Reserve University, Cleveland, Ohio 44106, USA;

[3]Oregon Institute of Occupational Health Sciences, Oregon Health & Science University, Portland, Oregon 97239, USA;

[4]Department of Internal Medicine, The Ohio State University, Columbus, Ohio 43210, United States

[5]Department of Endocrinology, Wuhan Central Hospital, Tongji Medical College, Huazhong University of Science and Technology, Wuhan, Hubei 430014, China;

[6]Department of Health Sciences, University of Missouri, Columbia, MO, United States

Abstract

Objective: Myeloid-related protein-14 (MRP14) and its binding partner MRP8 play an essential role in innate immune function and have been implicated in a variety of inflammatory diseases. However, the role of MRP14 in obesity-induced inflammation and insulin resistance is not well defined. This study investigated the role of MRP14 in macrophage-mediated adipose tissue inflammation and obesity-induced insulin resistance.

Subjects and Results: Wild-type (WT) and *Mrp14*$^{-/-}$ mice were fed a high-fat diet or normal chow for 12 weeks. Tissue-resident macrophages in both adipose tissue and liver from obese WT mice expressed higher levels of MRP14 in the visceral adipose fat and liver compared to the lean mice. *Mrp14*$^{-/-}$ mice demonstrated a significantly improved post-prandial insulin sensitivity, as

*Correspondence to: Jixin Zhong (jixin.zhong@case.edu); Address: 2103 Cornell Road, Wolstein Research Building RM 4525, Cleveland, OH 44106. Tel: 216-368-0126; Fax: 216-368-8898; or Shi Zhao (zhaoshiwuhan@126.com); Department of Endocrinology, Wuhan Central Hospital, Tongji Medical College, Huazhong University of Science and Technology, Wuhan, Hubei 430014, China.

AUTHOR CONTRIBUTIONS

C.X. and J.Z. researched data and wrote the manuscript. X.R. and Z.B. researched data. A.T., V.N., J.H., D.M., B.N., J.R., and J.A.D. contributed to clinical tissue collection. M.R., Z.B., S.Z., D.I.S., S.R., H.M., A.C.T., and X.R. contributed to discussion. J.Z., Z.B., M.R., A.C.T., and S.Z. reviewed and edited the manuscript. J.Z. is the guarantor of this work and, as such, had full access to all the data in the study and takes responsibility for the integrity of the data and the accuracy of the data analysis.

DUALITY OF INTEREST

No potential conflicts of interest relevant to this article were reported.

Supplementary Information Is Available At IJO's Website

measured by intraperitoneal glucose tolerance test and insulin tolerance testing. Macrophages secreted MRP14 in response to inflammatory stimuli such as LPS. Extracellular MRP8/14 induced the production of CCL5 and CXCL9. Deficiency of MRP14 did not affect macrophage proliferation, mitochondrial respiration, and glycolytic function, but *Mrp14*$^{-/-}$ macrophages showed a reduced ability to attract T cells. Depletion of the extracellular MRP14 reduced the T cell attracting ability of WT macrophages to a level similar to *Mrp14*$^{-/-}$ macrophages.

Conclusion: Our data indicates that MRP14 deficiency decreases obesity-induced insulin resistance and MRP8/14 regulates T cell recruitment through the induction of T cell chemoattractant production from macrophages.

Keywords

MRP14; Macrophages; Insulin sensitivity; Obesity; Inflammation

INTRODUCTION

Myeloid-related protein-14 (MRP14, S100A9) and its binding partner MRP8 (S100A8) are members of the S100 calcium-binding family of proteins which are predominantly expressed in, and released from, myeloid cells. MRP8/14 complex, also called calprotectin, is capable of sequestering transition metals[1]. MRP14 and MRP8 are expressed in phagocytic myeloid cells such as neutrophils, monocytes, dendritic cells, activated macrophages (but not non-activated macrophages), and platelets[2]. The expression of MRP8/14 is upregulated by oxidative stress, specific cytokines, and growth factors[3]. MRP14 is required for the stability of the MRP8 protein, as shown by *Mrp14*$^{-/-}$ mice not expressing MRP8 protein despite of the presence of MRP8 mRNA[4].

In addition to the metal sequestration function, MRP8/14 can also be released from the cells and serve as an alarmin to activate the immune system during inflammation[5, 6]. MRP8/14, an endogenous agonist of TLR4, plays an important role in sterile inflammation by activating TLR4/NF-κB signaling[5, 7–9]. Receptor for advanced glycation end-products (RAGE) has also been identified as a receptor for MRP8/14, promoting inflammation and cell growth in an NF-κB-dependent manner[10, 11]. Croce et al. reported that MRP14 deficiency in *ApoE*$^{-/-}$ mice showed a significant attenuation in atherosclerotic lesions and vasculitis. There was less macrophage accumulation in the plaque and lower levels of macrophage cytokines such as TNFα, IL-1β, MCP-1, and IL-12 in *Mrp14*$^{-/-}$ *ApoE*$^{-/-}$ mice[12].

Increasing evidence suggests a role for macrophage MRP8/14 in obesity and diabetes. The levels of MRP8/14 in circulation and in visceral adipose tissue was significantly increased in obese patients and positively correlated with monocyte/macrophage markers such as macrophage-specific antigen CD68 (CD68), monocyte chemotactic protein 1 (MCP1), and CD11b[13]. Mortensen et al. also reported that the plasma level of MRP8 was positively associated with the degree of obesity as indicated by body mass index (BMI)[14]. Later studies indicate that adipose MRP8/14 induces bone marrow myelopoiesis. This could be achieved either directly through activating RAGE on myeloid progenitor cells or indirectly via stimulating the IL-1 receptor on myeloid progenitor cells by inducing IL-1β release from

adipose tissue macrophages[15, 16]. Although hyperglycemia has been shown to induce MRP8/14 and myelopoiesis[16], it is not clear if MRP8/14 affects glucose metabolism and insulin resistance. In the current study, we provide direct evidence showing that MRP14 is involved in obesity-induced inflammation and insulin resistance. MRP14 expression, in insulin target organs such as the liver and adipose tissue, was increased in obese mice. Extracellular MRP8/14 upregulates the production of multiple chemokines such as CCL2, CCL5, and CXCL9 from macrophage, leading to an enhanced recruitment of T cells. Mrp14 deficient mice (*Mrp14*$^{-/-}$) lacking MRP8/14 complexes had a significantly increased insulin sensitivity, accompanied with reduced T cell infiltration.

MATERIALS AND METHODS

Reagents

Recombinant mouse MRP8/14 heterodimer was purchased from R&D Systems (Minneapolis, MN). Standard LPS 0111:B4 (from E. coli) was purchased from InvivoGen (San Diego, CA). Anti-phospho-NF-kB p65 ((Ser536), β-Actin (8H10D10) mouse antibody, and α/β-Tubulin antibody were obtained from Cell Signaling Technology (Danvers, MA). Caspase-1 p10 Antibody (M-20) was purchased from Santa Cruz Biotechnology (Santa Cruz, CA). The NLRP3/NALP-3 antibody was purchased from AdipoGen (San Diego, CA). μ-Slide chemotaxis and collagen I (rat tail) were obtained from IBIDI (Fitchburg, MA). RPMI-1640, heat-inactivated FBS, and penicillin/streptomycin (pen/strep) were purchased from Gibco (Gaithersburg, MD). Dynabeads® Protein G beads for immunoprecipitation were obtained from Life Technologies (Carlsbad, CA). All antibodies (CD4, clone GK1.5; CD11b, clone M1/70; CD19, clone1D3; CD8, clone SK1) used in flow cytometry were purchased from BioLegend (San Diego, CA). Click-iT™ EdU Alexa Fluor™ 647 Flow Cytometry Assay Kit was purchased from Invitrogen (Carlsbad, CA). Agilent Seahorse XF Glycolysis Stress Test Kit and Cell Mito Stress Test Kit were purchased from Agilent (North Billerica, MA). NE-PER Nuclear and Cytoplasmic Extraction Reagents, RANTES Mouse Instant ELISA™ Kit, CXCL9 Mouse ELISA Kit, Transwell® Costar Plates, and Pierce™ BCA Protein Assay Kit were purchased from ThermoFisher Scientific (Waltham, MA). Protease and Phosphatase Inhibitor Cocktail was obtained from Abcam (Cambridge, MA).

Animals

Mrp14$^{-/-}$ mice were generated in the laboratory of Nancy Hogg[17]. Tlr4Lps-d C3H mice were purchased from Jackson Laboratory. Eight-week old male *Mrp14*$^{-/-}$ and wild-type (WT) littermate controls were randomized to either a normal chow diet (ND) or a high fat diet (HFD), with 42% calories from fat (Harlan TD.88137), for 12 weeks. The mice were maintained in the animal facility at the Case Western Reserve University. All mice had a congenic C57BL/6 background and all procedures of this study were approved by the Institutional Animal Care and Use Committees at the Case Western Reserve University.

Intraperitoneal Glucose Tolerance Test (IPGTT) and Insulin Tolerance Test (IPITT)

For IPGTT, baseline blood glucose and body weights were measured after overnight fasting with free access to drinking water. Mice were i.p. injected with 2.0 g/kg body weight D-

glucose and blood glucose levels were measured at 30, 60, 90, and 120 min post injection using a Bayer Contour® glucometer.

For IPITT, baseline blood glucose and body weights were measured after 4 hours of fasting with free access to drinking water. Mice were i.p. injected with 0.75U/kg body weight insulin and blood glucose levels were measured at 30, 60, 90, and 120 min post injection using a Bayer Contour® glucometer.

Adipose Tissue & Liver Immunofluorescence

Epididymal fat and liver tissue from WT and *Mrp14*$^{-/-}$ mice (ND-fed or HFD-fed) were fixed in 10% Neutral Buffered Formalin and embedded in paraffin. Paraffin-embedded tissue sections (8μm) were used for detection of MRP14 by immunohistochemistry. Sections were blocked in 1% BSA for 1 hour after incubation in 1× Retrieve-All Antigen Unmasking Solution (Covance, Vienna, VA). MRP14 primary antibodies were diluted in blocking solution (10μg/ml) and applied for at least 1 hour at room temperature. Sections were then incubated with Texas Red-labeled anti-goat secondary antibody (10 μg/ml) diluted in 1% BSA in dark for 1 hour at room temperature. Resident macrophages were labeled with a FITC-conjugated rat anti-mouse CD11b antibody. Nuclei were stained with DAPI. Images were captured using a Leica microscope (DM2500) with a RETIGA EXi Fast 1394 camera (QIMAGING, Surrey, BC, Canada).

Bone Marrow Derived Macrophage Induction and Stimulation

Bone marrow cells from 8-to-12-week-old male WT or *Mrp14*$^{-/-}$ mice were cultured in RPMI-1640 supplemented with 10% FBS, 100 U/ml penicillin, 100 μg/ml streptomycin and 25 ng/mL M-CSF for 7 days to induce bone marrow derived macrophages (BMDMs). Mature macrophages were induced with LPS (1μg/mL, 16hr) at day 7. For MRP8/14 treatment, cells were stimulated with 3μg/mL recombinant mouse MRP8/14 heterodimer protein for 16hr. For culture supernatant collection, cells with or without LPS treatment at day 7 were washed with 1x PBS five times to remove LPS and cultured in fresh M-CSF containing medium. After 48 hours, cell culture media were then centrifuged at 3000 xg for 10 min and the supernatants were collected for experiments.

Analysis of mRNA Expression

Total RNA was extracted from BMDMs using Trizol® Reagent (Life Technologies, Grand Island, NY). cDNA was synthesized using High Capacity cDNA Reverse Transcriptase Kit (Life Technologies, Grand Island, NY) according to manufacturer's protocol. The amplification of target genes was used by a LightCycler® 480 SYBR Green I Master kit (Roche Applied Science, Indianapolis, IN). Gene expression was measured by quantitative real-time PCR performed on a LightCycler® 480 real-time PCR System (Roche Applied Science, Indianapolis, IN). The sequences of primers were shown in Table 1. Fold changes of mRNA levels were determined using the ΔΔCt method and normalized to β-actin.

Transwell® Assays

Transwell® assays were performed in Corning® Transwell® 24-well plate (6.5 mm diameter, 5 μM pore). To assess chemotactic effects of WT and *Mrp14*$^{-/-}$ BMDMs on T

cells, immature BMDMs (without LPS induction), and mature BMDMs (1 μg/mL LPS overnight treatment) were washed with 1x PBS for 3 times and incubated in a fresh serum free medium. After 24h, cell supernatant was collected for Transwell® assays. The splenocytes from WT mice were placed in the upper chamber (100μL suspension) and the lower chamber was filled with 600μL supernatants collected from BMDMs with indicated treatments. The Transwell® plates were then incubated in a 37°C CO_2 incubator for 5 hours. Cells were collected from both the upper and the lower chambers for cell counting and flow cytometric analysis after staining with cell population markers. The number of cells was counted three times for each sample and mean values and SD around the mean were calculated.

Flow Cytometry

Cells were gated based on viability (Life Technologies live/dead). Mouse antibodies (CD4, clone GK1.5; CD11b, clone M1/70; CD19, clone1D3; CD8, clone SK1; CD3 clone 2C11) were used in flow cytometry. Samples were collected on a Flowsight® imaging flow cytometer (Millipore) and analyzed with IDEAS software.

iBIDI® 3D Chemotaxis Assays and Migration in Collagen I Gels

Splenocytes isolated from WT mice were suspended with serum free RPMI medium. Cell concentration was 18×10^6/ml using ibidi's μ-Slide Chemotaxis 3D to reach a final concentration of 3×10^6/ml. For collagen preparation, 50 μL of spleen leukocytes (18 × 106/ml) were carefully mixed with 90 μL of rat tail type I collagen (5 mg/ml), 4 μL of $NaHCO_3$ (stock 7.5%), 50 μL of 1 × DMEM, 20 μL of 10 × DMEM and 5 μL of 1M NaOH. All solutions were previously placed on ice for 10 minutes. The final collagen I concentration in gel was 1.5 mg/ml. 6 μl of gel mix was then loaded in a μ-Slide Chemotaxis 3D and incubated at 37°C (5% CO_2) for 30 min to allow collagen polymerization. After incubation, the right chamber (chemoattractant-free side) was filled with 65μl chemoattractant-free medium and the left chamber (chemoattractant side) was filled with 65μl culture supernatant from BMDMs with indicated treatments. CCL19 (100 ng/mL) was used as a positive control. Time-lapse videos/images were recorded on a microscopy using a 10× objective. Cell migration was monitored for 12h. At least 30 cells over the whole period were tracked.

Chemokine Production

For chemokine secretion, BMDMs with indicated treatments were washed for three rinses with 1x PBS and cultured in fresh RPMI-1640 medium containing M-CSF (25 ng/mL). After 24 hours, supernatants were harvested after centrifugation. CCL5 and CXCL9 levels in supernatants were measured using ELISA kits as instructed by the manufacturers.

Immunoprecipitation

To deplete extracellular MRP8/14 in BMDMs supernatants, Protein G magnetic beads (50μl) were incubated with 5 μg anti-MRP14 antibody in 200μl PBS for 10 min. After washes, protein G beads conjugated with anti-MRP14 Ab were incubated with supernatants with rotation for 45 min at room temperature to allow extracellular MRP8/14 to bind to the

beads-Ab complex. The supernatants were then transferred to a clean tube for further treatment. The beads-Ab-Ag complex was washed 3 times using 200μl Washing Buffer and then eluted in 20μl Elution Buffer, followed by western blot analysis.

Glycolysis Rate and Mitochondrial Respiration Rate

For the measurements of Glycolysis rate and mitochondrial respiration rate, BMDMs were plated at the concentration of 150,000/well and accessed using the XF Glycolysis Stress Test Kit and the XF Cell Mito Stress Test Kit, according to the manufacturer's instructions. ECAR and OCR were measured using the Seahorse XF24 Extracellular Flux Analyzer (Seahorse Bioscience) as described previously[18]. The data was automatically calculated by Seahorse XF Glycolysis Stress Test and Cell Mito Stress Test Report Generator.

Cell Proliferation

BMDMs were treated with or without recombinant mouse MRP8/14 heterodimer protein (3μg/ml) and harvested for the detection of cell proliferation using Click-iT™ EdU Alexa Fluor™ 647 Flow Cytometry Assay Kit (ThermoFisher Scientific, Waltham, MA) as instructed. Cells were analyzed on a Flowsight® Imaging Flow Cytometer.

Statistical Analysis

All data are presented as mean ± SEM. P values of less than 0.05 were considered statistically significant. The statistical analysis of Student t test or one-way or two-way ANOVA and Bonferroni post hoc test where appropriate was completed using GraphPad Prism 5.

RESULTS

The expression of MRP14 increased in obesity

To examine the potential involvement of MRP14 in obesity-induced diabetes, we evaluated the expression of MRP14 in WT mice on normal chow diet (ND) vs high fat diet (HFD) for 12 weeks. As depicted in Figure 1A, HFD feeding increased adipocyte size and induced crown-like structures with massive macrophage infiltration in the visceral adipose tissue. There was an increased expression of MRP14 in HFD-fed mice compared to that of ND group, with MRP14 mainly expressed on CD11b-expressing macrophages (Figure 1A). Similarly, the HFD increased the expression of MRP14 in the liver (Figure 1B).

Loss of MRP14 improves insulin sensitivity

To test the role of MRP8/14 in the development of insulin sensitivity, WT and *Mrp14*$^{-/-}$ mice were fed a HFD or ND for 12 weeks. HFD feeding significantly increased body weight and fasting blood glucose in both WT and *Mrp14*$^{-/-}$ mice. However, there were no significant differences in body weight, tissue weight (epididymal fat, inguinal fat, liver, and soleus muscle), fasting blood glucose, or serum insulin between WT and *Mrp14*$^{-/-}$ mice (Figures 1C – 1E and Supplemental Figure 1). Interestingly, *Mrp14*$^{-/-}$ mice showed a markedly improved response to IPGTT and ITT (Figures 1F–1I). *Mrp14*$^{-/-}$ mice fed HFD had dramatically improved IPGTT and ITT responses. Indeed the blood glucose levels at the

time points of 30 min, 60 min, 90 min, and 120 min were similar between ND-fed and HFD-fed *Mrp14*$^{-/-}$ mice (Figures 1F & 1H). The areas under the curve of the IPGTT and ITT tests were also at similar levels between ND-fed and HFD-fed *Mrp14*$^{-/-}$ mice, although there was a trend to increase by 12 weeks of HFD feeding (Figures 1G & 1I). In addition, the expressions of *Cd4*, *Cd8*, *Il1b*, *Tnfa*, *Ccl2*, and *Cxcl9* were reduced, while M2 marker *Fizz1* was increased in the adipose tissue of HFD-fed *Mrp14*$^{-/-}$ mice (Figure 1J).

Effects of MRP14 on inflammatory gene expression in macrophage

Differentiation of macrophages has been suggested to alter expression of MRP81/4 raising the possibility that this may differentially affect function and expression of other cytokines. While no significant difference in *Tnfa* expression was observed between WT and *Mrp14*$^{-/-}$ undifferentiated bone marrow cells (Figure 2A), the expressions of *Il1b* (1±0.23 vs. 0.47±0.15 for WT vs. *Mrp14*$^{-/-}$, $p<0.001$) and *Il6* (1±0.27 vs. 0.39±0.13 for WT vs. *Mrp14*$^{-/-}$, $p<0.001$) were reduced significantly in *Mrp14*$^{-/-}$ mice (Figures 2B & 2C). Differentiated naïve macrophages (untreated BMDMs) showed the same results (Figures 2D–2F). In contrast, mature (LPS-treated) *Mrp14*$^{-/-}$ macrophages had reduced expressions of *Tnfa* and *Il1b*, but not *Il6* (Figures 2D–2F). Since the production of IL-1β is regulated by NLRP3 inflammasome, we next examined the expression of NLRP3 and activation of caspase-1. *Mrp14*$^{-/-}$ BMDMs had a lower level of *Nlrp3* mRNA expression, while treatment with exogenous MRP8/14 complex increased *Nlrp3* expression and there were no differences in *Nlrp3* expression between WT and *Mrp14*$^{-/-}$ macrophages after MRP8/14 treatment (Figure 2G). Consistent with this, protein levels of NLRP3 were also reduced in *Mrp14*$^{-/-}$ macrophages, compared with WT (Figure 2H). The active form of caspase-1 was increased after MRP8/14 treatment in both WT and *Mrp14*$^{-/-}$ macrophages, while LPS treatment increased the activation of caspase-1 in WT but not *Mrp14*$^{-/-}$ macrophages (Figures 2I & 2J). These data suggested that inflammatory stimuli such as LPS may induce activation of caspase-1 through the secretion of extracellular MRP14. To confirm this hypothesis, an anti-MRP14 antibody was used to pull-down MRP14 in the cell culture supernatant from untreated and LPS-treated WT macrophages. MRP14 was then precipitated from the supernatant and its levels quantified by Western Blot. The results indicated that LPS treatment significantly enhanced the release of MRP14 (Figure 2K). We next examined the effects of MRP14 on macrophage proliferation. WT and *Mrp14*$^{-/-}$ macrophages were treated with or without recombinant mouse MRP8/14 protein and cell proliferation of BMDMs was evaluated by Click-iT™ EdU Alexa Fluor™ 647 Flow Cytometry Assay. There was no significant difference in proliferation between WT and *Mrp14*$^{-/-}$ macrophages (Supplemental Figures 2A–2C). Similarly, treatment with extracellular MRP8/14 did not affect macrophage proliferation (Supplemental Figures 2A–2C). In consistency, there was also no significant difference in the expression of macrophage marker *CD11b* in the adipose tissue between WT and *Mrp14*$^{-/-}$ mice (Supplemental Figure 2D). These data indicate that MRP14 does not directly regulate macrophage proliferation. To examine a role for *Mrp14*$^{-/-}$ macrophages in regulation of macrophage metabolism, we evaluated cellular bioenergetics using a Seahorse XF24 Analyzer. There were no significant differences in glycolic capacity and mitochondrial respiration between WT and *Mrp14*$^{-/-}$ macrophages (Supplemental Figures 3A–3E)

Effects of MRP14 on chemokine production from macrophage

As depicted in Figures 3A–3E, *Ccl2* (1±0.05 vs. 0.56±0.09 for WT vs. *Mrp14*$^{-/-}$, p<0.001), *Ccl5* (1±0.31 vs. 0.16±0.12 for WT vs. *Mrp14*$^{-/-}$, p=0.01), *Cxcl9* (1±0.19 vs. 0.15±0.03 for WT vs. *Mrp14*$^{-/-}$, p<0.001), and *Cxcl*10 (1±0.18 vs. 0.35±0.07 for WT vs. *Mrp14*$^{-/-}$, p<0.001), were reduced significantly in *Mrp14*$^{-/-}$ mice, compared with those in WT mice. No difference in *Ccl22* expression was observed between WT and *Mrp14*$^{-/-}$ mice (1±0.19 vs. 0.79±0.22 for WT vs. *Mrp14*$^{-/-}$, p>0.05). Exogenous MRP8/14 treatment upregulated the expressions of *Ccl5* and *Cxcl9*, but not *Ccl2* and *Cxcl*10, suggesting that the downregulation of *Ccl2* and *Cxcl*10 in *Mrp14*$^{-/-}$ cells may not depend on extracellular MRP14 (Figures 3F–3J). Consistent with this, both naïve and mature BMDMs showed a similar expression pattern of *Ccl2*, *Ccl5*, and *Cxcl9* (Figures 3K–3M). ELISA assays confirmed the upregulation of CCL5 and CXCL9 in the culture supernatant (Figures 3N&3O). Since LPS treatment induces MRP14 release (Figures 3K), we wondered if MRP14 within the cell culture supernatant mediates the upregulation of these chemokines. To test this hypothesis, WT and *Mrp14*$^{-/-}$ macrophages were treated with or without culture supernatants from LPS-treated WT macrophages. *Ccl5* and *Cxcl9* mRNA expressions were then detected using real-time PCR. Supernatants from mature WT macrophages induced higher expressions of *Ccl5* and *Cxcl9* from both WT and *Mrp14*$^{-/-}$ cells, compared to those without supernatant treatment. More importantly, the differences between WT and *Mrp14*$^{-/-}$ were either diminished (*Cxcl9*) or reduced (*Ccl5*) after treatment of supernatants from LPS-treated macrophages which contained a significant amount of MRP14 (Figures 4A & 4B). Therefore, supernatant collected from mature macrophages was used for the following depletion experiments. To further confirm if the effect chemokine up regulation is mediated by MRP14, MRP14 was depleted from the supernatant using anti-MRP14 antibody-conjugated with Protein G magnetic beads. As shown in Figures 4C & 4D, the ability of WT mature macrophage-conditioned media to stimulate *Ccl5* and *Cxcl9* production was significantly reduced after MRP14 depletion. In contrast, MRP14 depletion did not affect the production of *Ccl5* and *Cxcl9* from *Mrp14*$^{-/-}$ supernatant-treated cells (Figures 4E & 4F). These results suggest that MRP14 within the macrophages (especially mature macrophages)-conditioned media promotes *Ccl5* and *Cxcl9* expression.

Extracellular Macrophage MRP14 enhances the ability to recruit T cells

CCL5 and CXCL9 are important chemokines that induce T cell recruitment. Given the role of macrophage MRP8/14 in inducing these cyotkines, we examined the effect of macrophage MRP-14 in T cell migration. Culture supernatants from WT or *Mrp14*$^{-/-}$ macrophages with or without LPS were collected from WT or *Mrp14*$^{-/-}$ macrophages and used in Transwell® assays of T cells. The migration of splenocytes towards supernatant from LPS-stimulated *Mrp14*$^{-/-}$ macrophage was reduced compared to that derived from WT cells, while no difference was observed in migration in response to supernatant from MRP8/14-treated WT and *Mrp14*$^{-/-}$ macrophages (Figure 5A). The migrated cells were then collected from the bottom wells of the Transwell® plate and used for flow cytometric analysis of cell components (Figures 5B–5H). Supernatant collected from mature *Mrp14*$^{-/-}$ macrophages attracted less T cells (including CD4+ and CD8+ T cells) and macrophages, but not B cells (Figures 5C–5H). Ibidi® 3D chemotaxis assay showed similar results that supernatant from *Mrp14*$^{-/-}$ macrophages had a reduced ability to attract splenocytes

(Figures 5I–5K). These results indicate that extracellular MRP14 may play a role in chemokine production and inflammatory cell recruitment. To exclude the direct effects of extracellular MRP8/14 on cell migration, MRP14 was depleted from the WT macrophage culture supernatant before the migration assay. As depicted in Figure 5L, depletion of MRP14 did not affect the ability of WT supernatants to attract splenocytes, suggesting the migration was induced by MRP14-mediated chemokine production rather than MRP14 itself. Consistent with these in-vitro observations, high fat diet feeding increased T cell infiltration in the liver of WT mice, but not in the liver of *Mrp14*$^{-/-}$ mice (Figures 5M).

MRP14 stimulates CCL5 and CXCL9 production through activating TLR4/NFκB pathway

Extracellular MRP8/14 has been shown to activate NFκB by binding to TLR4[19]. We therefore tested to see if MRP14-induced chemokine production depends on TLR4/ NFκB signaling. MRP8/14 treatment induced NFκB activation (Figure 6A). LPS-stimulated WT macrophages had a higher level of NFκB activation compared to *Mrp14*$^{-/-}$ macrophages, while depletion of extracellular MRP14 by antibody-mediated pull-down abolished this difference (Figure 6B & 6C). Furthermore, the upregulation of *Ccl5* and *Cxcl9* by exogenous MRP8/14 was abrogated by proteasome inhibitor MG132 which blocks activation of NF-κB (Figure 6D). MRP8/14 was unable to enhance the expression of *Ccl5* and *Cxcl9* in C3H mice with loss-of-function mutation of TLR4 (Figure 6E). These results indicate that MRP8/14-induced CCL5 and CXCL9 is dependent on TLR4/ NFκB activation.

DISCUSSION

Our work suggests an important role of MRP8/14 in insulin resistance and post-prandial glucose homeostasis in the absence of manifest changes in body weight or fasting glucose levels. In this study, we identified a new mechanism by which MRP14 plays a significant role in obesity-induced insulin resistance. MRP14 expression in the liver and adipose tissue was upregulated in obesity. MRP14 played an important role in regulation of expression of cytokines such as IL-β through an inflammasome pathway. This required the participation of extracellular MRP14. MRP14 did not play a role in macrophage proliferation and consistent with this did not influence macrophage metabolism or bioenergetics. We uncovered an unexpected paracrine role for extracellular macrophage MRP14 in T cell chemotaxis likely via up regulation of chemokine synthesis in macrophages such as CCL2, CCL5 and CXCL9.

It was recently demonstrated that MRP8/14 broadly regulates both innate and acquired immune responses, which contribute to the development of chronic inflammatory diseases, including obesity[15], cardiovascular disease[20], and Alzheimer's disease[21]. However, the role of MRP14 in obesity-induced inflammation and insulin resistance is not well defined. Our results provided direct evidence showing that unlike WT mice, *Mrp14*$^{-/-}$ mice were resistant to HFD-induced insulin resistance despite having similar levels of obesity. Deficiency of MRP14 improved responses to glucose tolerance test and insulin tolerance test in both ND- and HFD-fed mice. Interestingly, the serum insulin level in *Mrp14*$^{-/-}$ mice was similar as that in WT mice. This data suggests that *Mrp14*$^{-/-}$ mice have enhanced insulin sensitivity. Obesity-associated inflammation is widely considered as one of the major factors provoking insulin resistance and triggering Type 2 Diabetes[22]. HFD feeding significantly enhanced

insulin resistance in WT mice, while the responses to GTT and ITT were similar in ND-fed and HFD-fed *Mrp14*$^{-/-}$ mice. In addition, serveral inflammatory markers were reduced in HFD-fed *Mrp14*$^{-/-}$ mice. These results suggest that loss of MRP14 may prevent obesity-induced inflammation and insulin resistance. Ageing is also an important factor for chronic systemic inflammation[39]. We found that ND-fed *Mrp14*$^{-/-}$ mice also displayed a better response to both GTT and ITT. Considering the fact that those mice were 5-month old after 12-week diet treatment, it is possible that the improvement in the insulin resistance was a result of reduced age-associated inflammation. However, the role of MRP14 in ageing-related inflammation needs to be further investigated.

Macrophage accumulation in insulin target organs such as the liver and visceral adipose tissue (VAT) plays a key role in obesity-associated inflammation and insulin resistance[22, 23]. The recruitment of monocytes into inflammatory sites and subsequent differentiation into macrophages is a major event underlying the chronic systemic inflammation[37]_ENREF_2. Local macrophages are also able to proliferate and contribute to obesity-induced inflammation[38]. However, we did not observe a significant difference in adipose tissue macrophage number between WT and *Mrp14*$^{-/-}$ mice. The deficiency of MRP14 also did not impair macrophage proliferation. Overexpression of MCP-1 produced by adipocytes could promote the recruitment of macrophages to adipose tissue, thereby enhancing VAT inflammation and impairing insulin sensitivity[24]. In addition, the release of the MRP8/14 complex has also been reported to contribute to vildagliptin-associated liver dysfunction[25]. In our study, we observed an upregulation of MRP14 in both adipose tissue and liver tissue from obese mice. The NLRP3 inflammasome and its downstream IL-1β are important mediators of obesity-induced inflammation and insulin resistance[26]. It is suggested that MRP8/14 is able to induce NRLP3 inflammasome activation and IL-1β production via binding to TLR4[15]. In agreement with the findings by Nagareddy et al., we found that *Nlrp3* expression was lower in *Mrp14*$^{-/-}$ macrophages and MRP8/14 treatment increased *Nlrp3* expression to the same level in WT and *Mrp14*$^{-/-}$ macrophages. In addition, caspase-1 activation in macrophages was increased following stimulation with MRP8/14 or LPS. Interestingly, MRP8/14 stimulation, but not LPS stimulation, induced caspase-1 cleavage. In addition, LPS stimulation induced MRP14 secretion. This data suggests that MRP8/14 mediates the activation of NLRP3 inflammasome via LPS. Our data suggests that MRP14 may serve as a therapeutic target for disease conditions where NLRP3 inflammasome plays a crucial role, given the fact that NLRP3-inflammasome inhibition has been suggested as an effective approach for the treatment of inflammatory diseases[27, 28].

Chemokine-mediated recruitment of inflammatory cells, including macrophages and T cells, is a critical step in obesity-induced inflammation and insulin resistance[29–31]. In this study, we found that extracellular MRP14 induced the expression of *Ccl2*, *Ccl5*, and *Cxcl9* in macrophages. CCL2, also known as monocyte chemoattractant protein 1 (MCP-1), is a key chemokine that regulates the migration of monocytes/macrophages in diet-induced obesity and insulin resistance[32, 33]. Both CCL5 (also called regulated on activation, normal T cell expressed and secreted, RANTES) and CXCL9 (also called monokine induced by gamma interferon, MIG) are important chemoattractants for T cell recruitment[34]. Consistent with the chemokine expression profile, the supernatant from MRP14 deficient macrophages had less chemotactic activity for macrophages and T cells, but not B cells, in Transwell® assays.

MRP8/14 is actively released by macrophages in response to inflammatory stimuli and it serves as an innate alarmin to amplify immune response. Vogl et al. reported that LPS stimulation induces MRP8/14 secretion, which in turn augments LPS signaling through TLR45. In our study, we also found that LPS-treated macrophages secreted a significantly higher level of MRP14. In the following experiments, we confirmed that the extracellular MRP8/14 in turn acts on macrophages by activating the TLR4/NFκB pathway to stimulate the production of CCL5 and CXCL9. Supernatants from WT, but not *Mrp14*$^{-/-}$, macrophages stimulated the expression of *Ccl5*, and *Cxcl9*. This effect was abolished by the depletion of MRP14 from the supernatant, loss-of-function mutation of TLR4, or via NFκB inhibition.

Studies have indicated that there was a tight link between metabolism and macrophage function[35]. Bustos and Sobrino reported for the first time, that the inhibition of cytokine production in macrophages impaired macrophage metabolism by inactivating the glycolytic enzymes PFK1 and PFK2[36]. Our findings suggest that a deficiency of MRP14 did not change the macrophage mitochondrial respiration and glycolysis metabolic function. We also did not observe a direct effect of MRP14 on macrophage proliferation. This is consistent with the findings that MRP14 does not regulate myeloid cell development or differentiation in general[17].

In summary, our data demonstrates that MRP8/14 regulates the ability of macrophages to recruit leukocytes under inflammatory conditions, which may provide an insight into the involvement of macrophage/T cell inflammation in obesity-induced insulin resistance.

Supplementary Material

Refer to Web version on PubMed Central for supplementary material.

FUNDING

This work was supported by grants from National Institutes of Health (K01DK105108 and K99ES026241), National Natural Science Foundation of China (81670431, 31870906, 81370942, Y2110580, and 81101247), National Science and Technology Major Project (2016YFC1305803), American Heart Association (17GRNT33670485), American Association of Immunologists (CIIF-8745), and Hubei Regenerative Medicine Research Center.

REFERENCE

1. Sunahori K, Yamamura M, Yamana J, Takasugi K, Kawashima M, Yamamoto H, et al. The S100A8/A9 heterodimer amplifies proinflammatory cytokine production by macrophages via activation of nuclear factor kappa B and p38 mitogen-activated protein kinase in rheumatoid arthritis. Arthritis Res Ther. 2006;8:R69. [PubMed: 16613612]
2. Shimizu K, Libby P, Rocha VZ, Folco EJ, Shubiki R, Grabie N, et al.Loss of myeloid related protein-8/14 exacerbates cardiac allograft rejection. Circulation. 2011;124:2920–32. [PubMed: 22144572]
3. Hsu K, Champaiboon C, Guenther BD, Sorenson BS, Khammanivong A, Ross KF, et al.Anti-Infective Protective Properties of S100 Calgranulins. Antiinflamm Antiallergy Agents Med Chem. 2009;8:290–305. [PubMed: 20523765]
4. Manitz MP, Horst B, Seeliger S, Strey A, Skryabin BV, Gunzer M, et al. Loss of S100A9 (MRP14) results in reduced interleukin-8-induced CD11b surface expression, a polarized microfilament

system, and diminished responsiveness to chemoattractants in vitro. Mol Cell Biol. 2003;23:1034–43. [PubMed: 12529407]

5. Vogl T, Tenbrock K, Ludwig S, Leukert N, Ehrhardt C, van Zoelen MA, et al.Mrp8 and Mrp14 are endogenous activators of Toll-like receptor 4, promoting lethal, endotoxin-induced shock. Nat Med. 2007;13:1042–9. [PubMed: 17767165]
6. Rammes A, Roth J, Goebeler M, Klempt M, Hartmann M and Sorg C. Myeloid-related protein (MRP) 8 and MRP14, calcium-binding proteins of the S100 family, are secreted by activated monocytes via a novel, tubulin-dependent pathway. J Biol Chem. 1997;272:9496–502. [PubMed: 9083090]
7. Gross SR, Sin CG, Barraclough R and Rudland PS. Joining S100 proteins and migration: for better or for worse, in sickness and in health. Cell Mol Life Sci. 2014;71:1551–79. [PubMed: 23811936]
8. Sorci G, Riuzzi F, Giambanco I and Donato R. RAGE in tissue homeostasis, repair and regeneration. Biochim Biophys Acta. 2013;1833:101–9. [PubMed: 23103427]
9. Turovskaya O, Foell D, Sinha P, Vogl T, Newlin R, Nayak J, et al.RAGE, carboxylated glycans and S100A8/A9 play essential roles in colitis-associated carcinogenesis. Carcinogenesis. 2008;29:2035–43. [PubMed: 18689872]
10. Ghavami S, Rashedi I, Dattilo BM, Eshraghi M, Chazin WJ, Hashemi M, et al.S100A8/A9 at low concentration promotes tumor cell growth via RAGE ligation and MAP kinase-dependent pathway. J Leukoc Biol. 2008;83:1484–92. [PubMed: 18339893]
11. Gebhardt C, Riehl A, Durchdewald M, Nemeth J, Furstenberger G, Muller-Decker K, et al.RAGE signaling sustains inflammation and promotes tumor development. J Exp Med. 2008;205:275–85. [PubMed: 18208974]
12. Croce K, Gao H, Wang Y, Mooroka T, Sakuma M, Shi C, et al.Myeloid-related protein-8/14 is critical for the biological response to vascular injury. Circulation. 2009;120:427–36. [PubMed: 19620505]
13. Catalan V, Gomez-Ambrosi J, Rodriguez A, Ramirez B, Rotellar F, Valenti V, et al.Increased levels of calprotectin in obesity are related to macrophage content: impact on inflammation and effect of weight loss. Mol Med. 2011;17:1157–67. [PubMed: 21738950]
14. Mortensen OH, Nielsen AR, Erikstrup C, Plomgaard P, Fischer CP, Krogh-Madsen R, et al.Calprotectin--a novel marker of obesity. PLoS One. 2009;4:e7419. [PubMed: 19823685]
15. Nagareddy PR, Kraakman M, Masters SL, Stirzaker RA, Gorman DJ, Grant RW, et al.Adipose tissue macrophages promote myelopoiesis and monocytosis in obesity. Cell Metab. 2014;19:821–35. [PubMed: 24807222]
16. Nagareddy PR, Murphy AJ, Stirzaker RA, Hu Y, Yu S, Miller RG, et al.Hyperglycemia promotes myelopoiesis and impairs the resolution of atherosclerosis. Cell Metab. 2013;17:695–708. [PubMed: 23663738]
17. Hobbs JA, May R, Tanousis K, McNeill E, Mathies M, Gebhardt C,et al. Myeloid cell function in MRP-14 (S100A9) null mice. Mol Cell Biol. 2003;23:2564–76. [PubMed: 12640137]
18. Grunewald M, Johnson S, Lu D, Wang Z, Lomberk G, Albert PR, et al.Mechanistic role for a novel glucocorticoid-KLF11 (TIEG2) protein pathway in stress-induced monoamine oxidase A expression. J Biol Chem. 2012;287:24195–206. [PubMed: 22628545]
19. Xia C, Braunstein Z, Toomey AC, Zhong J and Rao X. S100 Proteins As an Important Regulator of Macrophage Inflammation. Front Immunol. 2017;8:1908. [PubMed: 29379499]
20. Ma LP, Haugen E, Ikemoto M, Fujita M, Terasaki F and Fu M. S100A8/A9 complex as a new biomarker in prediction of mortality in elderly patients with severe heart failure. Int J Cardiol. 2012;155:26–32. [PubMed: 21334078]
21. Wang A, Huen SC, Luan HH, Yu S, Zhang C, Gallezot JD, et al.Opposing Effects of Fasting Metabolism on Tissue Tolerance in Bacterial and Viral Inflammation. Cell. 2016;166:1512–1525 e12. [PubMed: 27610573]
22. Osborn O and Olefsky JM. The cellular and signaling networks linking the immune system and metabolism in disease. Nat Med. 2012;18:363–74. [PubMed: 22395709]
23. Weisberg SP, McCann D, Desai M, Rosenbaum M, Leibel RL and Ferrante AW Jr., Obesity is associated with macrophage accumulation in adipose tissue. J Clin Invest. 2003;112:1796–808. [PubMed: 14679176]

24. Kamei N, Tobe K, Suzuki R, Ohsugi M, Watanabe T, Kubota N, et al. Overexpression of monocyte chemoattractant protein-1 in adipose tissues causes macrophage recruitment and insulin resistance. J Biol Chem. 2006;281:26602–14. [PubMed: 16809344]
25. Asakura M, Karaki F, Fujii H, Atsuda K, Itoh T and Fujiwara R. Vildagliptin and its metabolite M20.7 induce the expression of S100A8 and S100A9 in human hepatoma HepG2 and leukemia HL-60 cells. Sci Rep. 2016;6:35633. [PubMed: 27759084]
26. Vandanmagsar B, Youm YH, Ravussin A, Galgani JE, Stadler K, Mynatt RL, et al.The NLRP3 inflammasome instigates obesity-induced inflammation and insulin resistance. Nat Med. 2011;17:179–88. [PubMed: 21217695]
27. Youm YH, Nguyen KY, Grant RW, Goldberg EL, Bodogai M, Kim D, et al.The ketone metabolite beta-hydroxybutyrate blocks NLRP3 inflammasome-mediated inflammatory disease. Nat Med. 2015;21:263–9. [PubMed: 25686106]
28. Goldberg EL, Asher JL, Molony RD, Shaw AC, Zeiss CJ, Wang C, et al.beta-Hydroxybutyrate Deactivates Neutrophil NLRP3 Inflammasome to Relieve Gout Flares. Cell Rep. 2017;18:2077–2087. [PubMed: 28249154]
29. Anderson EK, Gutierrez DA and Hasty AH. Adipose tissue recruitment of leukocytes. Curr Opin Lipidol. 2010;21:172–7. [PubMed: 20410821]
30. Carvalheira JB, Qiu Y and Chawla A. Blood spotlight on leukocytes and obesity. Blood. 2013;122:3263–7. [PubMed: 24065242]
31. Schmidt MI, Duncan BB, Sharrett AR, Lindberg G, Savage PJ, Offenbacher S, et al.Markers of inflammation and prediction of diabetes mellitus in adults (Atherosclerosis Risk in Communities study): a cohort study. Lancet. 1999;353:1649–52. [PubMed: 10335783]
32. Kawano Y, Nakae J, Watanabe N, Kikuchi T, Tateya S, Tamori Y, et al. Colonic Pro-inflammatory Macrophages Cause Insulin Resistance in an Intestinal Ccl2/Ccr2-Dependent Manner. Cell Metab. 2016;24:295–310. [PubMed: 27508875]
33. Xu H, Barnes GT, Yang Q, Tan G, Yang D, Chou CJ, et al.Chronic inflammation in fat plays a crucial role in the development of obesity-related insulin resistance. J Clin Invest. 2003;112:1821–30. [PubMed: 14679177]
34. Olson TS and Ley K. Chemokines and chemokine receptors in leukocyte trafficking. Am J Physiol Regul Integr Comp Physiol. 2002;283:R7–28. [PubMed: 12069927]
35. Galvan-Pena S and O'Neill LA. Metabolic reprograming in macrophage polarization. Front Immunol. 2014;5:420. [PubMed: 25228902]
36. Bustos R and Sobrino F. Stimulation of glycolysis as an activation signal in rat peritoneal macrophages. Effect of glucocorticoids on this process. Biochem J. 1992;282 (Pt 1):299–303. [PubMed: 1311557]
37. Gordon S and Taylor PR, Monocyte and macrophage heterogeneity. Nat Rev Immunol, 2005 5: p. 953–64. [PubMed: 16322748]
38. Flanagan SE, De Franco E, Lango Allen H, Zerah M, Abdul-Rasoul MM, Edge JA, et al. Analysis of transcription factors key for mouse pancreatic development establishes NKX2–2 and MNX1 mutations as causes of neonatal diabetes in man. Cell Metab. 2014;19, 146–154. [PubMed: 24411943]
39. Park MH, Kim DH, Lee EK, Kim ND, Im DS, Lee J,et al. Age-related inflammation and insulin resistance: a review of their intricate interdependency. Arch Pharm Res. 2014:37, 1507–1514. [PubMed: 25239110]

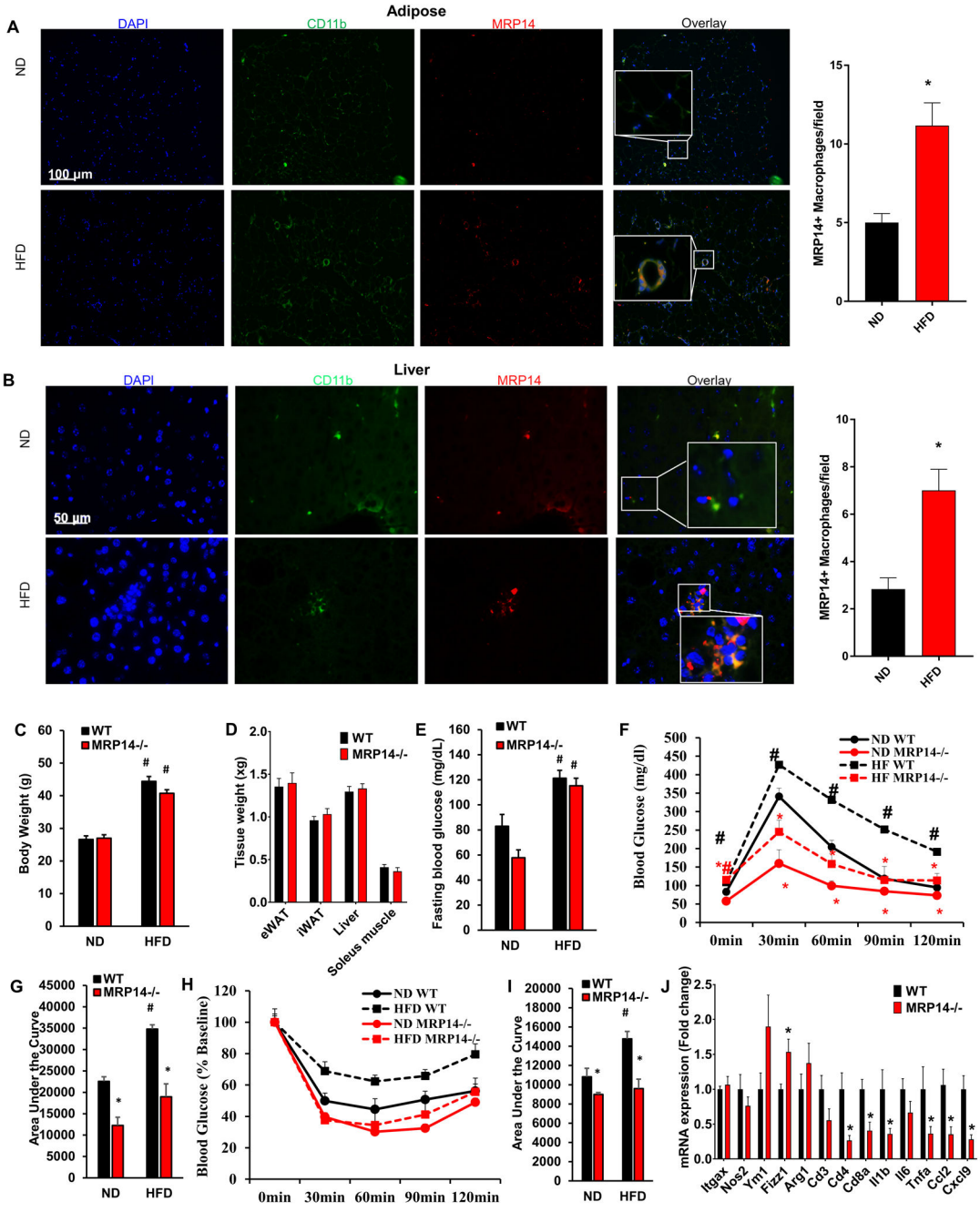

Figure 1. The MRP14 expression increased in obesity and insulin sensitivity in MRP14 deficient mice.

Epididymal fat pad (**A**) and liver (**B**) tissues were isolated from wild-type (WT) C57BL/6 mice on normal chow diet (ND) or high fat diet (HFD) and used for detection of MRP14 by immunofluorescence staining (mean ± SD, n = 8 per group). Resident macrophages were labeled in vivo using an FITC-conjugated rat anti-mouse CD11b antibody. Nuclei were stained with DAPI.WT mice and *Mrp14*$^{-/-}$ mice were fed ND or HFD for 12 weeks. Body weight (**C**), tissue weight (**D**), fasting blood glucose (**E**), and responses to IPGTT (**F**, blood glucose level before and after glucose challenge; **G**, area under the curve) or IPITT (**H**,

blood glucose level before and after insulin challenge; **I**, area under the curve) were measured. eWAT, epididymal white adipose tissue; iWAT, inguinal white adipose tissue. *, $p<0.05$ compared with WT; #, $p<0.05$ compared with ND.

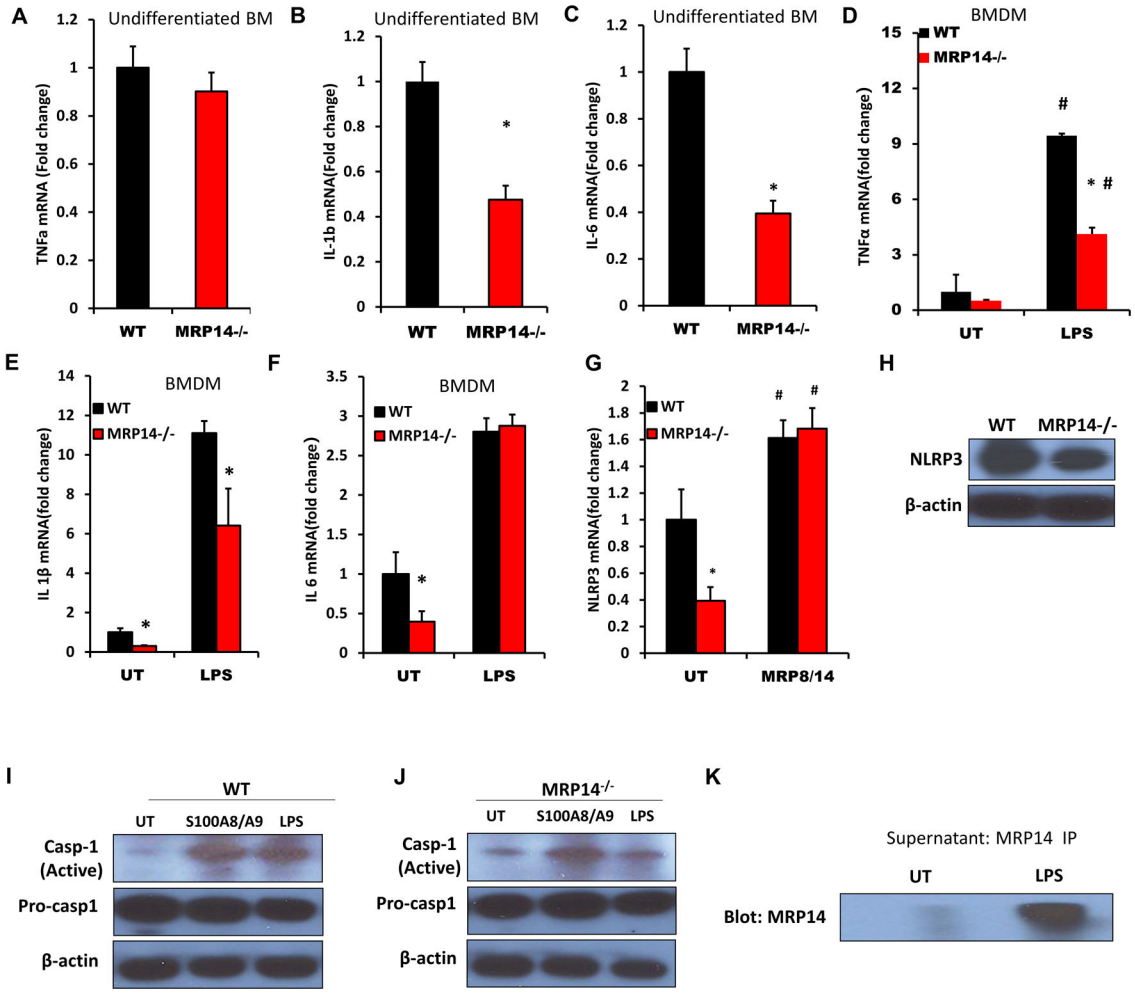

Figure 2. Effect of MRP14 depletion on expression of inflammatory cytokines.

Expressions of *Tnfa* (**A**), *Il1β* (**B**), and *Il6* (**C**) in bone marrow cells isolated from WT mice and *Mrp14*$^{-/-}$ mice were detected by real time PCR. WT or *Mrp14*$^{-/-}$ bone marrow derived macrophages (BMDMs) were either untreated (UT) or treated with 1μg/mL LPS for 24 hr. Expression of *Tnfa*(**D**), *Il1β*(**E**), and *Il6* (**F**) was then detected by real time PCR. **G** & **H**, WT and *Mrp14*$^{-/-}$ BMDMs were either untreated (UT) or stimulated with 1μg/mL LPS for 24 hr and the mRNA expression of *Nlrp3* was detected by real time PCR (**G**). Protein expressions of NLRP3 in untreated WT and *Mrp14*$^{-/-}$ BMDMs were confirmed by Western blotting (**H**). **I**, WT BMDMs were stimulated with 1μg/mL LPS, 3μg/mL MRP8/14 heterodimer, or vehicle control (1x PBS) for 24 hr. The levels of active caspase 1 and pro-caspase-1 were detected by Western blotting. **J**, Mrp14−/− BMDMs were stimulated with 1μg/mL LPS, 3μg/mL MRP8/14 heterodimer, or vehicle control (1x PBS) for 24 hr. The levels of active caspase-1 and pro-caspase-1 were detected by Western blotting. **K**, MRP14 in the supernatant collected from untreated or LPS-treated WT BMDMs was detected by Western blotting. *, $p<0.05$ compared with WT; #, $p<0.05$ compared with UT.

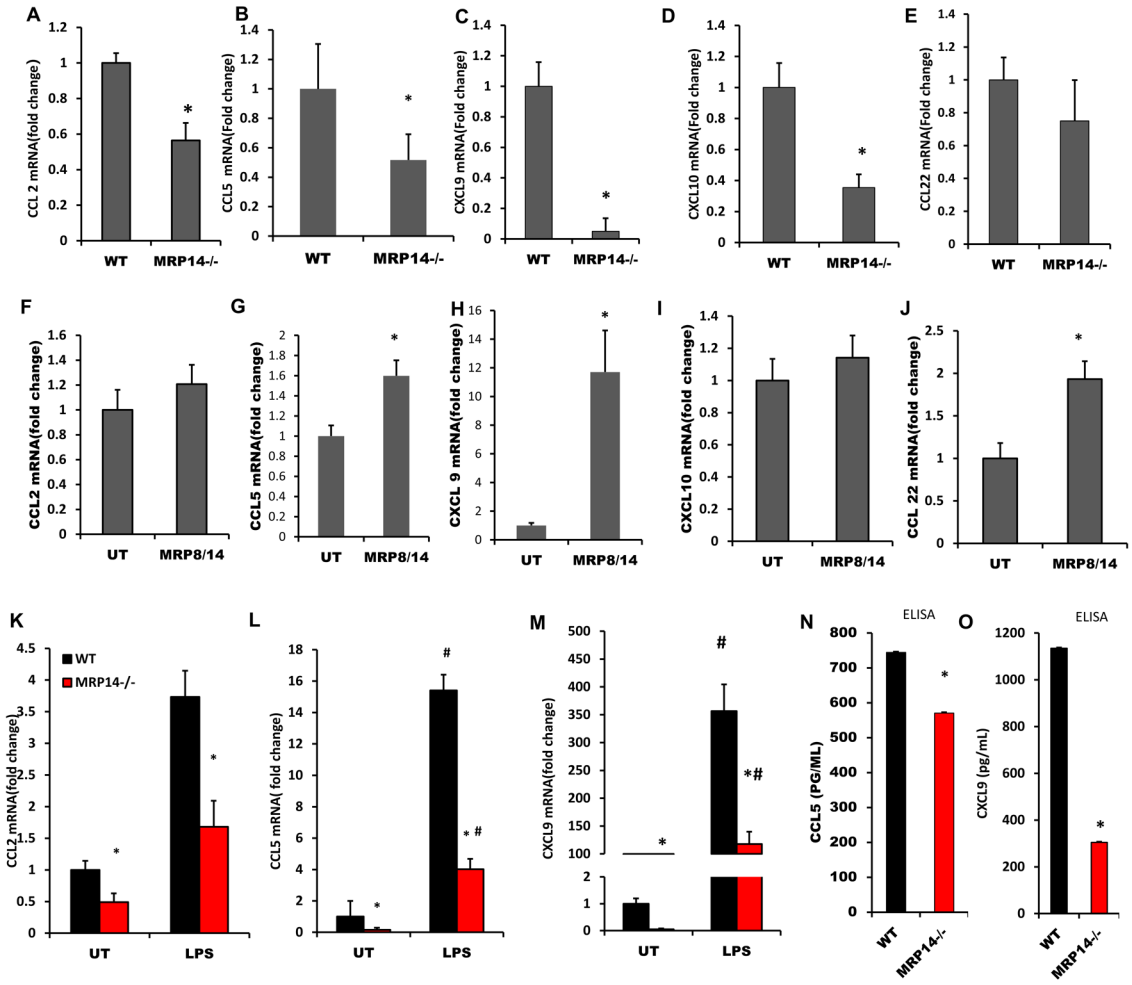

Figure 3. MRP14 enhanced chemokine production by macrophages.

A-E, Undifferentiated bone marrow cells from WT or *Mrp14*$^{-/-}$ mice were used for the real time PCR detection of *Ccl2* (**A**), *Ccl5* (**B**), *Cxcl9* (**C**), *Cxcl10* (**D**), and *Ccl22* (**E**). **F-J**, WT or *Mrp14*$^{-/-}$ bone marrow derived macrophages (BMDMs) were stimulated with recombinant MRP8/14 heterodimer (3μg/mL) for 16 hrs and the mRNA expressions of *Ccl2* (**F**), *Ccl5* (**G**), *Cxcl9* (**H**), *Cxcl10* (**I**), and *Ccl22* (**J**) were detected by real time PCR. **K-M**, mRNA expressions of *Ccl2* (**K**), *Ccl5* (**L**), and *Cxcl9* (**M**) were detected in untreated (UT) or LPS-treated WT or *Mrp14*$^{-/-}$ BMDMs. **N-O**, Culture supernatant of WT or *Mrp14*$^{-/-}$ BMDMs was used for the ELISA detection of CCL5 (**N**) and CXCL9 (**O**) production. *****, $p<0.05$ compared with WT; #, $p<0.05$ compared with UT.

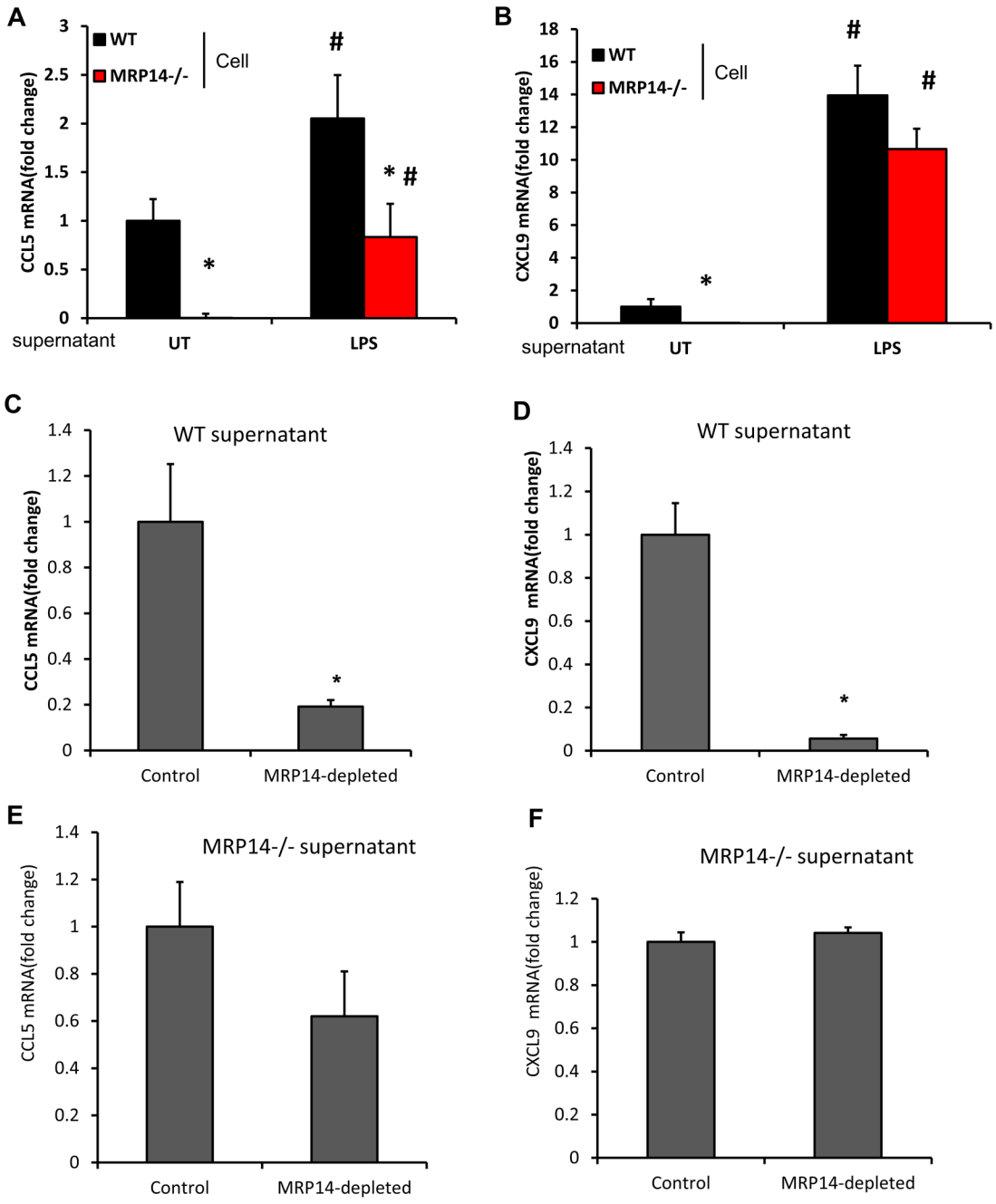

Figure 4. Effects of extracellular MRP14 on CCL5 and CXCL9 expression.

A & **B**, Culture supernatant harvested from untreated (UT) or LPS-treated WT macrophages was used to treat WT or *Mrp14*$^{-/-}$ BMDMs. After 16 hrs of treatment, cells were subjected to real time PCR detection of *Ccl5* (**A**) and *Cxcl9* (**B**). **C-F**, Protein G magnetic beads conjugated with anti-MRP14 antibody was used to deplete extracellular MRP8/14 in supernatants collected from mature WT (**C** & **D**) or *Mrp14*$^{-/-}$ (**E** & **F**) macrophages. Unconjugated beads were used as a control. Culture supernatants with or without MRP14 depletion were then used to treat WT BMDMs, mRNA levels of *Ccl5* (**C** & **E**) and *Cxcl9* (**D** & **F**) a*****, $p<0.05$ compared with WT; #, $p<0.05$ compared with UT.

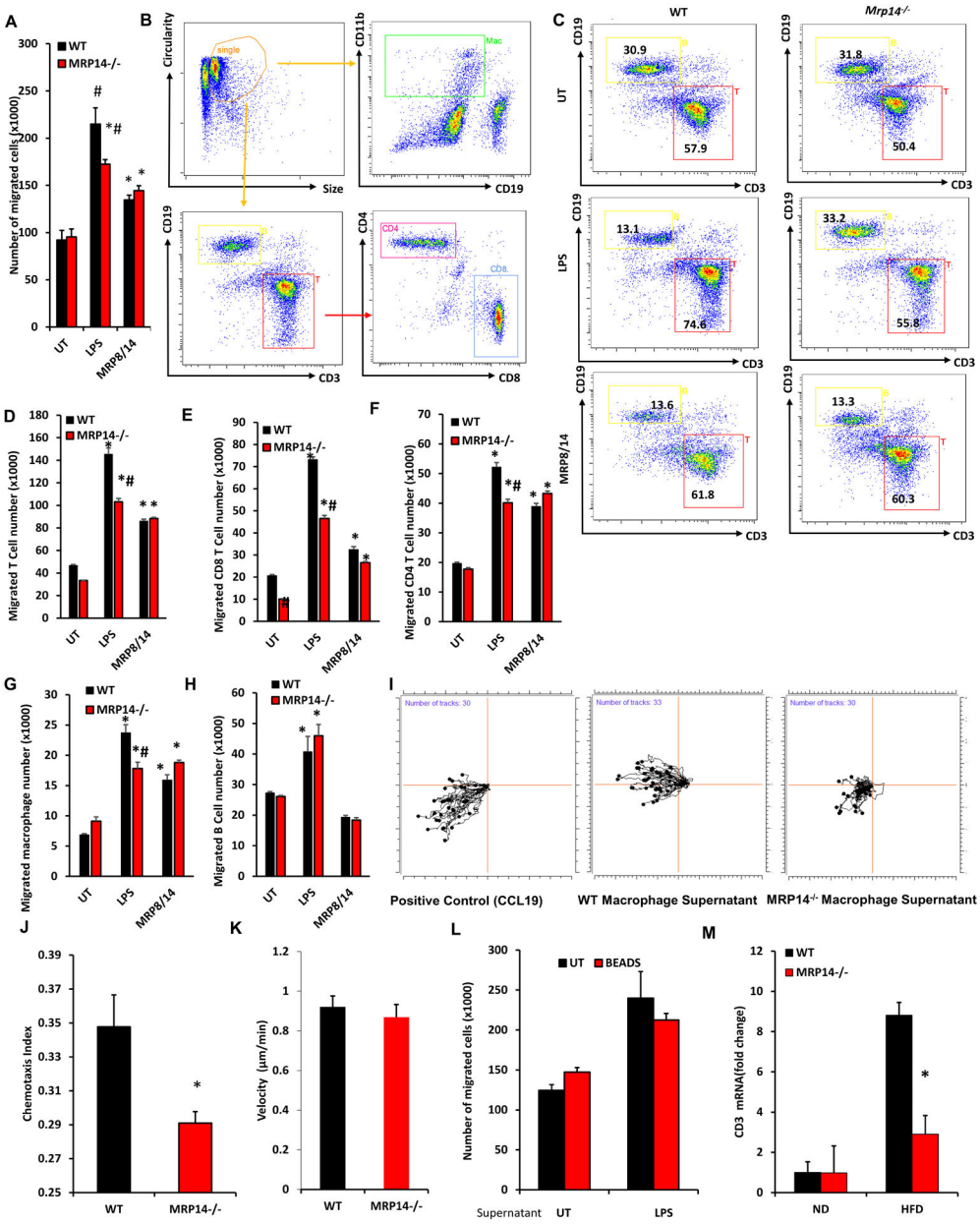

Figure 5. Effects of MRP14 on the ability of macrophage to recruit T cells.

A-H, BMDMs from WT and *Mrp14*$^{-/-}$ mice were treated with LPS (1 μg/ml, 24 hrs) or MRP8/14 heterodimer (3μg/mL, 24 hrs) and cell supernatant was collected for Transwell® assay. Leukocytes from the spleen of WT mice were placed in the insert of a 12-well Transwell® plate and the culture supernatant from treated WT and *Mrp14*$^{-/-}$ macrophages were placed in the bottom well. The total number of cells migrated into the bottom well was counted (A). The migrated cells were used for flow cytometric detection of different populations (B, gating strategy; C, representative dot plots showing T cell and B cell percentage) and the number of migrated T cells (D), CD8 T cells (E), CD4 T cells (F), CD11b^{+} CD19^{-} macrophages (G), and CD19^{+} B cells (H) were calculated. **I-K**, iBIDI® Chemotaxis Assays. The same culture supernatants described in Figure 6A were also used

for the iBIDI 3D Chemotaxis Assays representative plots (I), chemotaxis index (J), and migration velocity were shown. **L**, Protein G magnetic beads conjugated with anti-MRP14 antibody was used to deplete extracellular MRP8/14 in BMDMs supernatants. Culture supernatants with or without depletion of MRP14 were used for Transwell® assay. Depletion of MRP14 did not affect the migration, suggesting MRP14 does not directly induced cell migration. **M**, Expression of T cell marker Cd3e in the liver tissues of WT or *Mrp14*$^{-/-}$ mice was shown. *****, $p<0.05$ compared with WT; $^{\#}$, $p<0.05$ compared with UT.

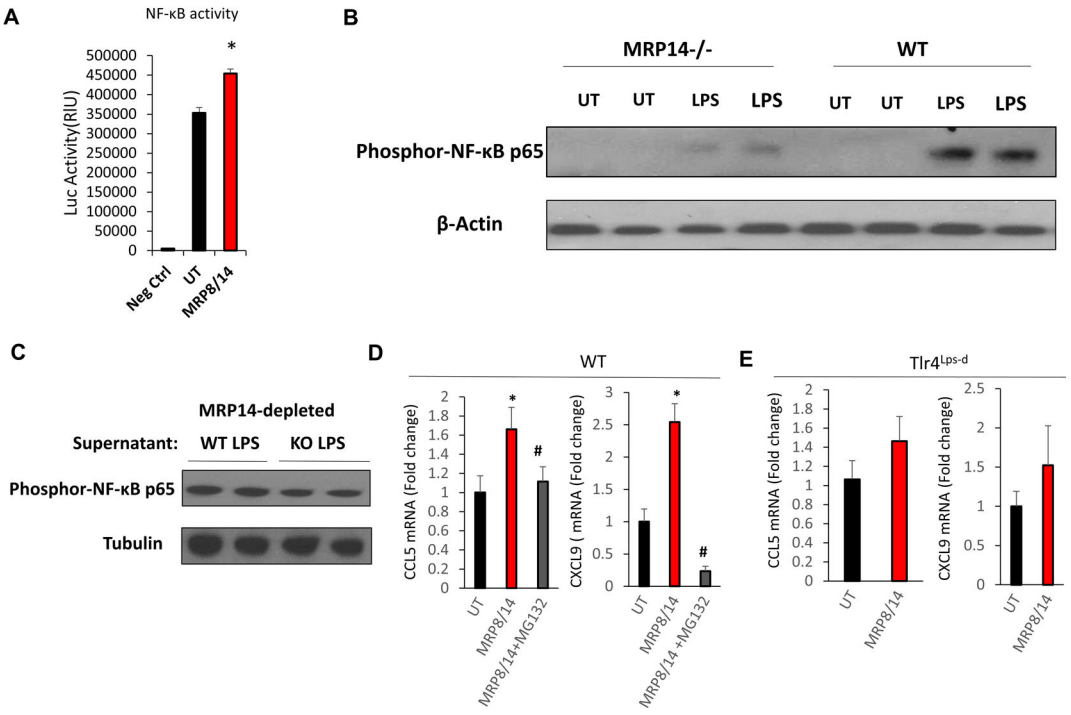

Figure 6. MRP14 upregulated CCL5 and CXCL9 via TLR4/NFκB-dependent mechanism.

A, HEK 293 cells were transfected with NF-κB luciferase reporter plasmids. After 24 hrs of transfection, cells were then treated with MRP8/14 recombination protein (3μg/ml) or vehicle control for 6 hrs. Luciferase activities were determined using a luciferase assay kit. Data shown is the mean + SD (n = 3). **B**, WT and *Mrp14*$^{-/-}$ BMDMs were either untreated (UT) or treated with LPS, phosphor-NF-κB p65 was detected by Western Blot. **C**, MRP14 was depleted from the WT or *Mrp14*$^{-/-}$ BMDM culture supernatants and the supernatant was used to treat WT BMDMs. Phosphor-NF-κB p65 was then detected by Western Blot. **D** & **E**, WT (**D**) and *Tlr4*$^{Lps\text{-}d}$ (**E**) BMDMs with or without pretreatment of 5μM MG132 were treated with MRP8/14 for 16 hrs. *Ccl5* and *Cxcl9* expressions were detected by real time PCR. *, $p<0.05$ compared with UT; #, $p<0.05$ compared with MRP8/14 treatment group.

Table 1.

Real-time PCR primer sequence

Target gene	Primer sequence (5′ to 3′)
TNFα	Forward CAACGGCATGGATCTCAAAGAC Reverse AGATAGCAAATCGGCTGACGGT
CCL-2	Forward TCACCTGCTGCTACTCATTCACCA Reverse TACAGCTTCTTTGGGACACCTGCT
CXCL-5	Forward CTCACCATCATCCTCACTGC Reverse AAATACTCCTTGACGTGGGC
CXCL9	Forward TCTGCATCAGTGACGGTAAAC Reverse TGAAGGGCACAGTTTGGAG
CXCL-10	Forward TCCGCTGTTCTTTTCCTCTTG Reverse GAGGGATTTGTAGTGGATCGTG
IL-1 β	Forward ATGGCAGAGATCGAGAAAGC Reverse GCACCTTTGTCGTTTATGAGC
IL-6	Forward TTCAACCAGCACCAGACAG Reverse AGACCACATCCACAAACATCC
CCL22	Forward ACAGATGACATGGTGAAGACG Reverse TCGTTCTTGTGTAGTTCCAGTG
NLRP3	Forward CCCATGAGTTCCCTTAAGCTG Reverse AGTGCCCAGTCCAACATAATC
Caspase-1	Forward TTCAACATCTTTCTCCGAGGG Reverse CACCTCTTTCACCATCTCCAG
CD3	Forward TGCCACGACATTCACAGAG Reverse ATGAGTTCCACCTTGCAGAG
β-actin	Forward TGTGATGGTGGGAATGGGTCAGAA Reverse TGTGGTGCCAGATCTTCTCCATGT